DOI: 10.1002/asia.200800036

Homolytic S–S Bond Dissociation of 11 Bis(thiocarbonyl)disulfides R-C(=S)–S–S–C(=S)R and Prediction of A Novel Rubber Vulcanization Accelerator

Adrian Matthew Mak,[a] Ralf Steudel,[b] and Ming Wah Wong*[a]

Abstract: The structures and energetics of eight substituted bis(thiocarbonyl)disulfides $(RCS_2)_2$, their associated radicals $RCS_2^{\bullet}$, and their coordination compounds with a lithium cation have been studied at the G3X(MP2) level of theory for R = H, Me, F, Cl, OMe, SMe, NMe_2, and PMe_2. The effects of substituents on the dissociation of $(RCS_2)_2$ to $RCS_2^{\bullet}$ were analyzed using isodesmic stabilization reactions. Electron-donating groups with an unshared pair of electrons have a pronounced stabilization effect on both $(RCS_2)_2$ and $RCS_2^{\bullet}$. The S–S bond dissociation enthalpy of tetramethylthiuram disulfide (TMTD, R = NMe_2) is the lowest in the above series (155 kJ mol^{-1}), attributed to the particular stability of the formed $Me_2NCS_2^{\bullet}$ radical. Both $(RCS_2)_2$ and the fragmented radicals $RCS_2^{\bullet}$ form stable chelate complexes with a Li^+ cation. The S–S homolytic bond cleavage in $(RCS_2)_2$ is facilitated by the reaction $[Li(RCS_2)_2]^+ + Li^+ \rightarrow 2[Li(RCS_2)]^{\bullet +}$. Three other substituted bis(thiocarbonyl) disulfides with the unconventional substituents R = OSF_5, Gu^1, and Gu^2 have been explored to find suitable alternative rubber vulcanization accelerators. Bis(thiocarbonyl)-disulfide with a guanidine-type substituent, $(Gu^1CS_2)_2$, is predicted to be an effective accelerator in sulfur vulcanization of rubber. Compared to TMTD, $(Gu^1CS_2)_2$ is calculated to have a lower bond dissociation enthalpy and smaller associated barrier for the S–S homolysis.

Keywords: ab initio calculations · bond energy · ligand design · radical ions · sulfur

Introduction

The vulcanization of natural or synthetic rubber is one of the most important industrial processes in our civilization. This process essentially involves the cross-linking of individual rubber polymer chains (e.g., *cis*-polyisoprene) via sulfide and disulfide bridges, making the overall material mechanically stronger but still elastic, as well as resistant to chemical attack. The discovery of vulcanization using elemental sulfur has been credited to Charles Goodyear, but it has recently been discovered that Mesoamericans have achieved this method of rubber vulcanization as early as 1600 B.C.[1] Nowadays, a vast number of reagents associated with sulfur vulcanization of rubber polymers have been developed. These include dithiocarbamates, thiurams, thiourea, thiazoles, and sulfenamides;[2] their chemical structures are shown in Scheme 1. Among these, mercaptobenzothiazoles (MBT) and the thiurams are most effective for rubber vulcanization.

Our recent study on the accelerator tetramethylthiuram disulfide (TMTD) showed that its S–S bond dissociation enthalpy (150 kJ mol^{-1}) is significantly lower than that of the corresponding trisulfide (TMTT; 190 kJ mol^{-1}), based on high-level G3X(MP2) calculations.[3] To gain further insight into the effect of substituents on the S–S bond dissociation energy, we have carried out a systematic study of a series of bis(thiocarbonyl)disulfides, R–C(=S)–S–S–C(=S)–R, using high-level ab initio calculations. A number of conventional univalent substituents (R), namely H, Me, F, Cl, OMe, SMe, NMe_2, and PMe_2, were examined. The better known bis(thiocarbonyl)disulfides are those with R = alkyl/aryl,[4] OMe,[5] SMe,[6,7], and NMe_2.[8] Less is known about the

---

[a] Dr. A. M. Mak, Prof. Dr. M. W. Wong
Department of Chemistry
National University of Singapore
3 Science Drive 3, Singapore 117543
Fax: (+65) 7791 691
E-mail: chmwmw@nus.edu.sg

[b] Prof. Dr. R. Steudel
Institut für Chemie
Technische Universität Berlin, Sekr. C2
10623 Berlin (Germany)

Supporting information for this article, including the total energies and atomic coordinates of all optimized structures [(B3LYP/6-31G-(2df,p)] (Table S1), is available on the WWW under http://www.chemasianj.org or from the author.

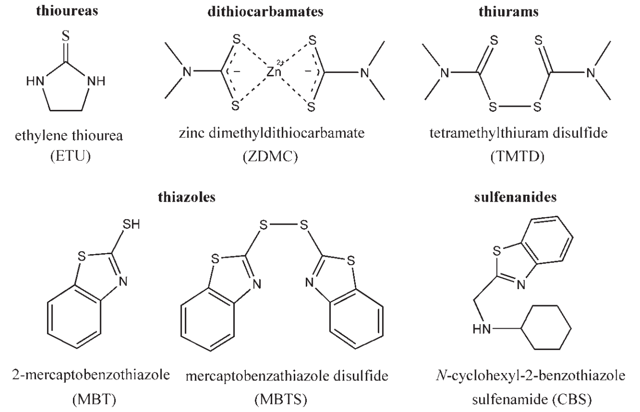

Scheme 1. Examples of sulfur vulcanization reagents available commercially.

chlorine-substituted derivative (R = Cl),[9] and no references have been found for R = F and PMe_2. Except for the well-characterized TMTD,[10] no experimental structure determinations of these compounds have been published to date. However, theoretical structure calculations have been reported for R = H (at the HF/STO-3G level)[4] for R = OMe (CNDO level)[11] and for R = NMe_2 (G3X(MP2) level).[3] An important goal of our work was to obtain structural and thermochemical data for the seven poorly characterized molecules mentioned above at a high level of theory for the first time.

Many coordination compounds are known which contain the disulfide TMTD as a ligand or anionic derivatives obtained by reductive cleavage of its S–S bond.[12] To systematically investigate the ligand properties of the neutral species $(RCS_2)_2$ and the radicals $RCS_2^{\bullet}$ that form as a result of S–S bond homolysis, the lithium cation is used as a model metal cation for ligand coordination. The small Li^+ cation allows for a high level of theory to be used in quantum chemical calculations. Since the binding energies of Li^+ complexes towards a large number of Lewis bases are linearly related to those of other cations such as Na^+ and Mg^{2+},[13] the use of Li^+ as a model cation is justifiable.

As shown in our previous work, the $Me_2NCS_2^{\bullet}$ radical is remarkably stable, attributed to the effective delocalization of the π electrons and the spin density over the four-center NCS_2 framework.[3] However, the S–S bond dissociation enthalpy (BDE) for TMTD is still endothermic by 155.1 $kJ\,mol^{-1}$ at the G3X(MP2) level.[3] In industrial rubber vulcanization, activators such as zinc oxide are added to facilitate S–S bond breaking by the coordination of TMTD to zinc. The binding of small sulfur-containing compounds to zinc oxide clusters has recently been investigated by Steudel et al., with the result that the binding energies of S_6, Me_2S_2, MeSH, and Me_2S to a cubane-like Zn_4O_4 cluster are exothermic by −60.7 to −106.7 $kJ\,mol^{-1}$.[14] Zinc oxide, however, is an environmental pollutant that displays ecotoxicity[15] and the inhalation of zinc oxide can result in severe pulmonary conditions.[16,17] In an effort to find ways that can further stabilize the $RCS_2^{\bullet}$ radical and, hence, reduce the reliance on zinc oxide activators, some unconventional substituents R were considered based on their strong electron-donating or -withdrawing ability as well as their ability to promote resonance-stabilized structures (see Scheme 2). The electron-withdrawing ability of the OSF_5 group has been demonstrated by its strong conjugate acid $HOSF_5$,[18] and the two cyclic guanidine-type substituents (hereby denoted Gu^1 and Gu^2) have been noted for their strong basicity[19] as well as ability to form numerous resonance-stabilized structures that result in the stabilization of the $RCS_2^{\bullet}$ radical. Thus, the hypothetical bis(thiocarbonyl)disulfides with these novel substituents were also examined theoretically.

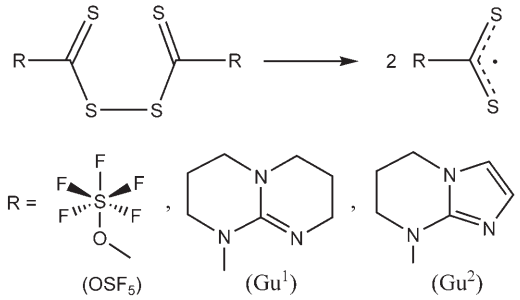

Scheme 2. The homolytic dissociation of $(RCS_2)_2$ using novel substituents (R).

Computational Details

The structures and energies of the disulfides $(RCS_2)_2$, radicals $RCS_2^{\bullet}$, and their lithiated complexes for R = H, Me, F, Cl, OMe, SMe, NMe_2, and PMe_2 were examined at the G3X(MP2) level of theory.[20] The G3X(MP2) method corresponds effectively to energies calculated at the QCISD(T)/G3XL//B3LYP/6-31G(2df,p) level, based on basis set additivity evaluated at the MP2 level. A spin–orbit correction term and a high-level empirical correction term are included in the final energy. Three important changes in the G3X(MP2) theory from the G3(MP2)[21] theory are important for the proper description of the sulfur-rich molecules studied: 1) the use of B3LYP/6-31G(2df,p) geometry; 2) the use of B3LYP/6-31G(2df,p) zero-point vibrational energy scaled by an empirical factor of 0.9854; 3) an addition of a g polarization function to the G3Large basis set for second-row atoms at the Hartree–Fock level.[20] Structures of the larger bis(thiocarbonyl)disulfides $(F_5SOCS_2)_2$, $((Gu^1)CS_2)_2$, and $(Gu^2)CS_2)_2$ and their associated radicals $F_5SOCS_2^{\bullet}$, $(Gu^1)CS_2^{\bullet}$, and $(Gu^2)CS_2^{\bullet}$ were optimized at the B3LYP/6-31G(d) level. Energy calculations for these three systems were then carried out at the MP2(fc)/6-311+G(d,p) level of theory based on the B3LYP/6-31G(d)-optimized structures. Singlet biradical transition states corresponding to the homolytic S–S bond cleavage were optimized at this level of theory as well, using the UHF formalism and the mixing of the HOMO and LUMO to destroy α and β spatial symmetries. The RHF formalism was employed for all closed-shell species, and the UHF formalism was employed for all open-shell and singlet diradical species. Frequency calculations were carried out to determine the nature of the stationary points calculated. Those with all frequencies real correspond to local minima, while those with one and only one imaginary frequency correspond to transition-state structures. For all investigated species, a charge density analysis was performed using the natural bond orbital (NBO)[22] approach based on the B3LYP/6-31G(2df,p) wavefunction. NBO atomic charges of small molecules have recently been demonstrated to agree well with experimental values obtained from X-ray diffraction data.[23] All calculations were carried out using the GAUSSIAN 03[24] and MOLPRO 2002[25] suites of programs.

Results and Discussion

Bis(thiocarbonyl)disulfides with the Conventional Substituents R = H, Me, F, Cl, OMe, SMe, NMe_2, and PMe_2

We first examined the effect of several univalent substituents on the S–S bond dissociation reaction of bis(thiocarbonyl)disulfide. The typical structures of $(RCS_2)_2$, $RCS_2^{\bullet}$, $[Li(RCS_2)_2]^+$, $[Li(RCS_2)]^{\bullet +}$, and triplet $[(RCS_2)Li(S_2CR)]^+$, together with their atom labelings, are shown in Figure 1.

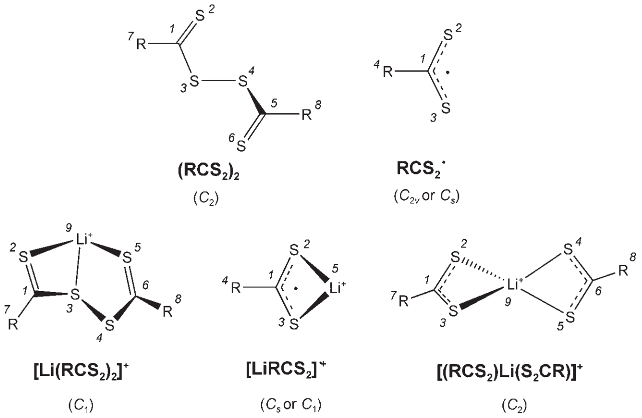

Figure 1. Typical structures of $(RCS_2)_2$, $RCS_2^{\bullet}$, $[Li(RCS_2)_2]^+$, $[Li(RCS_2)]^{\bullet +}$ and triplet $[(RCS_2)Li(S_2CR)]^+$ according to reference [3]. Molecular symmetry is indicated in parentheses.

Table 1. Selected calculated (B3LYP/6-31G(2df,p)) bond lengths (in Å) of $(RCS_2)_2$. Average experimental values[26] for C–R bond lengths are included for comparison.

R	C1–S3	C1=S2 (=C5=S6)	S3–S4	C1–R7 (=C5–R8)	Average exptl C–R
H	1.756	1.614	2.065	1.095	1.092 (C–H)
Me	1.785	1.622	2.049	1.512	1.501 (C–C)
F	1.785	1.603	2.045	1.331	1.327 (C–F)
Cl	1.775	1.604	2.058	1.767	1.752 (C–Cl)
OMe	1.809	1.628	2.034	1.327	1.405 (C–O)
SMe	1.806	1.626	2.037	1.755	1.803 (C–S)
NMe_2	1.840	1.650	2.023	1.347	1.428 (C–N)
PMe_2	1.783	1.631	2.059	1.844	1.858 (C–P)

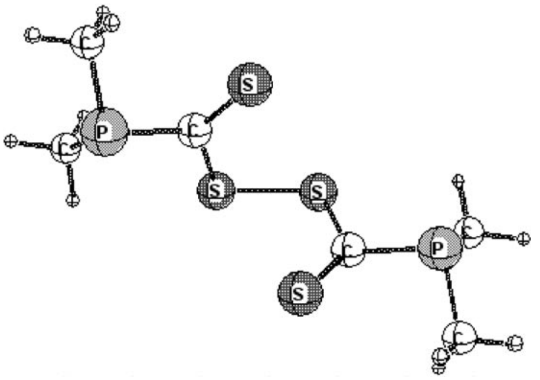

Figure 2. The B3LYP/6-31G(2df,p)-optimized structure of $(Me_2PCS_2)_2$, showing the lack of planarity at the C_2PCS_2 framework.

Selected calculated structural parameters of the substituted bis(thiocarbonyl)disulfides $(RCS_2)_2$ with R = H, Me, F, Cl, OMe, SMe, NMe_2, and PMe_2 are presented in Table 1. Consistent with our previous studies on tetramethylthiuram disulfide (TMTD),[3] the most stable conformers of substituted $(RCS_2)_2$ are of C_2 symmetry. In the case of $(Me_2PCS_2)_2$, the C_2PCS_2 skeleton is not planar but pyramidal at the phosphorus atom (Figure 2), unlike TMTD, which has an almost planar C_2NCS_2 framework. This is not unexpected, as phosphorus prefers a high s-orbital character of the lone-pair electrons, and, hence, shows a reluctance to undergo s,p hybridization to form a planar coordination at P.[27,28] The C=S bond lengths in $(RCS_2)_2$ range from 1.603 Å for the fluorine substituent to 1.650 Å for the dimethylamino group. As expected, a shorter central S–S bond is associated with longer C=S bonds. The S–S bond lengths range from 2.023 Å for the Me_2N group to 2.065 Å for the parent compound (R = H). For R = H, Me, F, and Cl, the calculated C–R distances are slightly longer than the average experimental value.[26] This trend is reversed for the electron-donating substituents with a lone pair of electrons, namely R = OMe, SMe, NMe_2, and PMe_2. The largest deviations occur for R = OMe and NMe_2 (bond shortening of 0.076 and 0.081 Å, respectively), which is indicative of the delocalization of π electrons within the OCS_2 and NCS_2 frameworks. The extent of delocalization becomes less pronounced for the third-row analogues R = SMe and PMe_2, with the difference in bond lengths at 0.048 and 0.014 Å, respectively. In general, a shorter C–R bond length correlates with a longer C=S bond (Table 1). This structural feature can readily be understood in terms of the contribution of the dipolar resonance form (see Scheme 3). Thus, for substituents with an unshared pair of electrons, the C–R distances are significantly shorter while the C=S bond lengths are longer.

The radicals $RCS_2^{\bullet}$ are either of C_{2v} (R = H, F, Cl, NMe_2) or C_s symmetry (R = Me, OMe, SMe, PMe_2). The calculated C–S and C–R bond lengths are given in Table 2. The $RCS_2^{\bullet}$ radical is resonance stabilized, as evidenced from the C–S

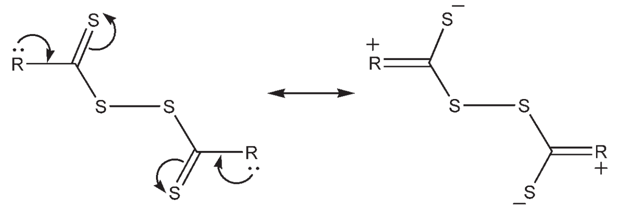

Scheme 3. Resonance hybrid of bis(thiocarbonyl)disulfide $(RCS_2)_2$.

Table 2. Selected calculated (B3LYP/6-31G(2df,p)) bond lengths (in Å) of $RCS_2^{\bullet}$.

Substituent (R)	C1–R4	C1–S2, C1–S3
H	1.089	1.665
Me	1.495	1.674
F	1.315	1.659
Cl	1.740	1.659
OMe	1.315	1.683,[a] 1.679[b]
SMe	1.728	1.685,[c] 1.679[d]
NMe_2	1.335	1.700
PMe_2	1.816	1.683

[a] *trans* with respect to O–CH_3. [b] *cis* with respect to O–CH_3. [c] *trans* with respect to S–CH_3. [d] *cis* with respect to S–CH_3.

bond lengths of 1.659 to 1.700 Å, intermediate between the typical length of a C–S single bond (1.803 Å) and a C=S double bond (1.584 Å). For all the substituents considered, the C–R bonds are also slightly shorter than those in the corresponding dimer $(RCS_2)_2$, suggesting an increased extent of delocalization of π electrons into the attachment atom of the R group (i.e., C for Me, O for OMe, N for NMe_2). The spin density plot of the $HCS_2^{\bullet}$ radical shown in Figure 3 indicates that the $RCS_2^{\bullet}$ radicals are essentially of σ type, with the unpaired spin density located in both sulfur atoms. Thus, $RCS_2^{\bullet}$ is best described as a resonance hybrid of two sulfur-centered σ radicals.

In Table 3 the homolytic S–S bond dissociation energies (ΔE°, ΔH°_{298}, and ΔG°_{298}) of bis(thiocarbonyl)disulfides $(RCS_2)_2$, calculated at the G3X(MP2) level of theory, are tabulated. Most of the investigated $(RCS_2)_2$ molecules have homolytic S–S bond dissociation enthalpies (BDE) in excess of 190 kJ mol^{-1}. However, TMTD (R = NMe_2) has a substantially lower BDE of 155.1 kJ mol^{-1}. What is the origin of the dramatic reduction of BDE in TMTD? To further shed light on the effect of substituents (R) on the S–S BDE, we have computed the stabilization of $(RCS_2)_2$ and $RCS_2^{\bullet}$ with respect to the parent molecules $(HCS_2)_2$ and $HCS_2^{\bullet}$ using the two isodesmic reactions[30,31] shown in Equations (1) and (2).

$$(RCS_2)_2 + 2\,CH_4 \rightarrow (HCS_2)_2 + 2\,CH_3R \qquad (1)$$

$$RCS_2^{\bullet} + CH_4 \rightarrow HCS_2^{\bullet} + CH_3R \qquad (2)$$

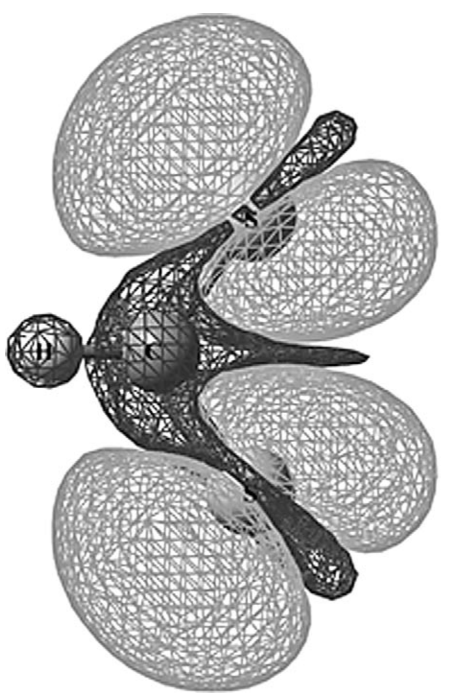

Figure 3. UB3LYP/6-31G(2df,p) spin density plot of the $HCS_2^{\bullet}$ radical.

Table 3. ΔE°, ΔH°_{298}, and ΔG°_{298} values for the homolytic S–S bond dissociation reaction $(RCS_2)_2 \rightarrow 2\,RCS_2^{\bullet}$, calculated at the G3X(MP2) level of theory.

Substituent (R)	ΔE° [kJ mol^{-1}]	ΔH°_{298} [kJ mol^{-1}]	ΔG°_{298} [kJ mol^{-1}]
H	210.0	210.8	158.4
Me	193.0	193.0	139.1
F	190.2	190.0	137.1
Cl	206.9	215.2	161.9
OMe	206.8	206.5	153.1
SMe	196.6	195.7	146.5
NMe_2	155.6	155.1	100.3
PMe_2	199.1	198.9	141.7

Table 4. Calculated substituent stabilization energies[a] (kJ mol^{-1}) of $(RCS_2)_2$, $RCS_2^{\bullet}$, and S–S bond dissociation of $(RCS_2)_2$ based on isodesmic reactions.

Substituent (R)	$(RCS_2)_2$[b]	$RCS_2^{\bullet}$[c]	$(RCS_2)_2 \rightarrow 2\,RCS_2^{\bullet}$[d]
Me	129.3	73.2	17.0
F	133.6	76.7	19.8
Cl	115.4	59.2	3.1
OMe	234.4	118.8	3.2
SMe	184.2	98.8	13.4
NMe_2	251.9	153.1	54.4
PMe_2	142.6	76.8	11.0

[a] G3X(MP2) level of theory. [b] Based on Equation (1). [c] Based on Equation (2). [d] Computed from the relative stabilization energy of (RCS_2) and $2\,RCS_2^{\bullet}$.

The results given in Table 4 illustrate that both $(RCS_2)_2$ and $RCS_2^{\bullet}$ are stabilized by electron-withdrawing and electron-donating substituents. The extent of stabilization is particularly large for the electron-donating substituents with an unshared pair of electrons, such as OMe and NMe_2. The substituent stabilization effect of S–S homolysis depends on the relative stabilizing effect of the disulfide and its related radicals. In general, the combined stabilization energies of two RCS$_2^\bullet$ radicals are larger than the stabilization energy of corresponding disulfide (RCS$_2$)$_2$. As a consequence, there is a net increase in the stabilization energy for the S–S bond dissociation process (Table 4). The differential stabilization effect is very large for the dimethylamino substituent (R = NMe$_2$). Hence, the remarkably lower BDE of TMTD is attributed mainly to the significant stability of the Me$_2$NCS$_2^\bullet$ radical. Our finding here confirms the idea that substituents which stabilize the RCS$_2^\bullet$ radical by electron-donating and resonance effects are promising systems with low BDE.

Coordination of Li$^+$ to the Disulfides and the Radicals

The effect of metal ion coordination on the S–S BDEs of the eight bis(thiocarbonyl)disulfides was investigated using the Li$^+$ ion as a model cation. As with TMTD,[3] the preferred Li$^+$ coordination sites for (RCS$_2$)$_2$ are located at the terminal sulfur atoms instead of the attachment atom of the substituent. Generally, coordination of (RCS$_2$)$_2$ to Li$^+$ occurs through three favorable Li$^+$⋯S interactions with a reduction in molecular symmetry from C_2 to C_1 (see Figure 1). Selected calculated geometrical parameters of the [Li(RCS$_2$)$_2$]$^+$ complexes are presented in Table 5. All three Li$^+$⋯S interactions for all eight complexes studied occur at distances below 2.8 Å, and are thus expected to be bonding interactions with a electron density maximum along their path.[29] For the radicals [Li(RCS$_2$)]$^{\bullet+}$, the Li$^+$ ion is slightly out of the plane defined by C1–S2–S3 (see Figure 1). As already mentioned in our previous work with the Me$_2$NCS$_2^\bullet$ radical, Li$^+$ is at a compromised position between two forces: the ion-dipole attraction which is maximum in the CS$_2$ plane, and a covalent bond interaction with the sulfur 3p lone pairs perpendicular to the CS$_2$ plane. This positioning of the Li$^+$ ion can also be seen in the triplet [(RCS$_2$)Li(S$_2$CR)]$^+$ complexes. The Li$^+$ ion is coordinated to two RCS$_2^\bullet$ radicals through their terminal sulfur atoms in a tetrahedral manner. An overall C_2 molecular symmetry is observed for these complexes (see Figure 1). Selected geometrical parameters for the [Li(RCS$_2$)]$^{\bullet+}$ and triplet [(RCS$_2$)Li(S$_2$CR)]$^+$ complexes are shown in Tables 6 and 7.

Table 5. Selected calculated (B3LYP/6-31G(2df,p)) bond lengths (in Å) of [Li(RCS$_2$)$_2$]$^+$.

Substituent	Li–S2	Li–S3	Li–S5	S3–S4	C1–R7	C6–R8
H	2.510	2.541	2.456	2.087	1.091	1.091
Me	2.474	2.483	2.433	2.080	1.489	1.508
F	2.506	2.561	2.451	2.073	1.296	1.308
Cl	2.494	2.515	2.456	2.076	1.701	1.722
OMe	2.452	2.496	2.410	2.062	1.291	1.301
SMe	2.441	2.482	2.409	2.064	1.704	1.725
NMe$_2$	2.371	2.517	2.349	2.069	1.323	1.332
PMe$_2$	2.423	2.476	2.399	2.086	1.791	1.824

Table 6. Selected calculated (B3LYP/6-31G(2df,p)) bond lengths (in Å) of [Li(RCS$_2$)]$^{\bullet+}$.

Substituent	Li–S2	Li–S3	C1–S2	C1–S3	C1–R7
H	2.521	2.521	1.675	1.675	1.089
Me	2.479	2.479	1.690	1.690	1.484
F	2.513	2.513	1.679	1.679	1.287
Cl	2.504	2.504	1.684	1.684	1.689
OMe	2.463	2.450	1.704	1.708	1.282
SMe	2.456	2.439	1.705	1.713	1.691
NMe$_2$	2.419	2.419	1.725	1.725	1.310
PMe$_2$	2.431	2.431	1.712	1.712	1.771

Table 7. Selected calculated (B3LYP/6-31G(2df,p) bond lengths (in Å) of triplet [(RCS$_2$)Li(S$_2$CR)]$^+$.

Substituent	Li–S2 (=Li–S5)	Li–S3 (=Li–S4)	C1–S2 (=C6–S5)	C1–S3 (=C6–S4)	C1–R7 (=C6–R8)
H	2.585	2.584	1.671	1.672	1.089
Me	2.551	2.550	1.685	1.685	1.486
F	2.567	2.568	1.675	1.675	1.290
Cl	2.565	2.564	1.678	1.679	1.695
OMe	2.516	2.539	1.701	1.698	1.288
SMe	2.513	2.541	1.706	1.698	1.697
NMe$_2$	2.505	2.506	1.717	1.718	1.314
PMe$_2$	2.520	2.523	1.702	1.702	1.782

Table 8. ΔH°_{298} and ΔG°_{298} values (in kJ mol^{-1}) for the coordination of (RCS$_2$)$_2$ and RCS$_2^\bullet$ to Li$^+$, calculated at the G3X(MP2) level of theory.

Substituent	Li$^+$ + (RCS$_2$)$_2$→[Li(RCS$_2$)$_2$]$^+$		Li$^+$ + (RCS$_2$)$^\bullet$→[Li(RCS$_2$)]$^{\bullet+}$	
	ΔH°_{298}	ΔG°_{298}	ΔH°_{298}	ΔG°_{298}
H	−166.3	−131.4	−101.6	−72.1
Me	−199.3	−163.7	−122.7	−93.7
F	−137.6	−103.2	−80.6	−50.6
Cl	−152.6	−117.5	−101.5	−71.3
OMe	−219.1	−184.4	−138.9	−108.7
SMe	−227.0	−188.9	−142.6	−111.8
NMe$_2$	−284.9	−243.8	−181.1	−149.0
PMe$_2$	−223.6	−192.0	−139.9	−109.9

Coordination of (RCS$_2$)$_2$ or RCS$_2^\bullet$ to Li$^+$ is always exothermic and exergonic, as shown in Table 8. For R = NMe$_2$ (i.e., TMTD), the Li$^+$ binding energy to the disulfide and its radical is highest, while in the case for R = F it is the lowest. The low binding energy for (FCS$_2$)$_2$ and FCS$_2^\bullet$ can be explained by the highly electronegative fluorine atom drawing electron density away from the CS$_2$ moiety, resulting in less pronounced ion-dipole attraction. This is evidenced in the calculated NBO charges on fluorine of −0.292 for (FCS$_2$)$_2$ and −0.283 for FCS$_2^\bullet$; the NBO charge on the sulfur atoms of (FCS$_2$)$_2$ are 0.078 and 0.226, and those on FCS$_2^\bullet$ are 0.164. Although the attachment atoms for R = OMe and NMe$_2$ are also highly electronegative, the contribution of electron density from the methyl groups to the oxygen and nitrogen atoms leads to effective back-donation of electron density from oxygen and nitrogen lone pairs to the CS$_2$ moiety, resulting in less positive NBO charges on the sulfur atoms and a more favorable Li$^+$⋯S interaction. The NBO charges on sulfur atoms for the cases R = OMe and NMe$_2$ are: for (MeOCS$_2$)$_2$, −0.040 and 0.212, for MeOCS$_2^\bullet$ (C_s symmetry) 0.057 and 0.137, for (Me$_2$NCS$_2$)$_2$, −0.115 and 0.172, and for Me$_2$NCS$_2^\bullet$, 0.040. The NBO charges for the above species were evaluated at the B3LYP/6-31G(2df,p) level.

Subsequent Li^+-mediated S–S homolytic bond cleavage in $(RCS_2)_2$ can occur via a number of possible modes. These can also be facilitated by additional Li^+ ions or the incorporation of elemental sulfur to form bis(thiocarbonyl) oligosulfides, followed by formation of disulfidic, trisulfidic, and polysulfidic radicals. The following three modes, shown in Equations (3)–(5) are considered in this study:

$$[Li(RCS_2)_2]^+ \rightarrow [Li(RCS_2)]^{\cdot +} + (RCS_2)^{\cdot} \tag{3}$$

$$[Li(RCS_2)_2]^+ \rightarrow [(RCS_2)Li(S_2CR)]^+ \tag{4}$$

$$[Li(RCS_2)_2]^+ + Li^+ \rightarrow 2\,[Li(RCS_2)]^{\cdot +} \tag{5}$$

As evidenced in Table 9, calculated gas-phase enthalpies and free energies of the above three reactions are generally endothermic. The S–S BDEs for Equation (3) are highly endothermic by more than 200 kJ mol^{-1} for all substituents. The fluorine substituent shows the lowest enthalpy (247.0 kJ mol^{-1}) and the highest is that for the methoxy substituent (286.7 kJ mol^{-1}). The enthalpies for Equation (3) show small variation across different substituents, and are higher than those for Equations (4) and (5). The lower enthalpies for Equation (4) compared to Equation (3) show that it is more favorable for S–S bond dissociation with associated curve crossing to occur while the $(RCS_2)_2$ ligand is still chelated to the Li^+ ion. Another explanation for the lower enthalpy is the formation of an additional $Li^+\cdots S$ contact, which provides further stabilization of the fragmented Li^+ adduct. The trend for the S–S BDE for Equation (4) is different from that for Equation (3). The highest S–S BDE for Equation (5) is that for the parent compound (R = H) at 198.3 kJ mol^{-1}, and the lowest is that of TMTD ($R = NMe_2$) at 127.0 kJ mol^{-1}. The addition of Li^+ ions aid the process of S–S bond dissociation further, shown in the enthalpies for Equation (5). The enthalpy trend for Equation (5) is similar to that for Equation (4), again with the parent compound having the highest reaction enthalpy of 173.9 kJ mol^{-1} and TMTD having the lowest reaction enthalpy of 78.2 kJ mol^{-1}.

Table 9. ΔH°_{298} and ΔG°_{298} values (kJ mol^{-1}) for the reactions $[Li(RCS_2)_2]^+ \rightarrow [Li(RCS_2)]^{\cdot +} + (RCS_2)^{\cdot}$, $[Li(RCS_2)_2]^+ \rightarrow [(RCS_2)Li(S_2CR)]^+$, and $[Li(RCS_2)_2]^+ + Li^+ \rightarrow 2\,[Li(RCS_2)]^{\cdot +}$, calculated at the G3X(MP2) level of theory.

Substituent	$[Li(RCS_2)_2]^+ \rightarrow [Li(RCS_2)]^{\cdot +} + (RCS_2)^{\cdot}$		$[Li(RCS_2)_2]^+ \rightarrow [(RCS_2)Li(S_2CR)]^+$		$[Li(RCS_2)_2]^+ + Li^+ \rightarrow 2\,[Li(RCS_2)]^{\cdot +}$	
	ΔH°_{298}	ΔG°_{298}	ΔH°_{298}	ΔG°_{298}	ΔH°_{298}	ΔG°_{298}
H	275.5	217.7	198.3	174.2	173.9	145.6
Me	269.6	209.2	176.7	151.1	146.9	115.5
F	247.0	189.7	183.7	161.7	166.4	139.1
Cl	266.2	208.0	187.3	164.1	164.6	136.6
OMe	286.7	228.9	180.2	157.3	147.9	120.2
SMe	280.2	223.7	175.2	154.6	137.6	111.9
NMe_2	259.3	195.4	127.0	100.3	78.2	46.4
PMe_2	282.5	223.8	173.9	151.2	142.6	113.9

Breaking of the S–S bonds in bis(thiocarbonyl)disulfides seems to be unfavorable, with S–S BDEs being generally endothermic by more than 100 kJ mol^{-1}. The addition of Li^+ ions helps facilitate this process by forming energetically favorable $Li^+\cdots S$ interactions. Taking the enthalpy values from Tables 8 and 9, Li^+-mediated S–S bond dissociation by Equation (5) is the most favorable for TMTD ($R = NMe_2$) with ΔH°_{298} and ΔG°_{298} values being highly exothermic and exergonic, by −206.7 and −197.5 kJ mol^{-1}, respectively. In a very recent study, we have examined the role of Zn_4O_4 as an activator for the S–S bond dissociation of TMTD.[32]

Bis(thiocarbonyl)disulfides with the Unconventional Substituents $R = OSF_5$, Gu^1, and Gu^2

Bis(thiocarbonyl)disulfides $(RCS_2)_2$ with the conventional substituents R = H, CH_3, F, Cl, OMe, SMe, and PMe_2 have larger S–S bond dissociation energies (BDEs) than TMTD, and, thus, there remains a reliance on a metal cation to facilitate S–S homolysis. Therefore, it is intriguing to determine whether other suitable substituents can lower further the S–S BDE of TMTD by either increasing or lowering the electron density at the S–S bond. To this end, we have explored three additional bis(thiocarbonyl)disulfides with the unconventional substituents $R = OSF_5$, Gu^1, and Gu^2 (Scheme 2). The two cyclic guanidine-type pyrimidines[33] are stronger electron-donating substituents than NMe_2,[19] while the OSF_5 group is known to be one of the most electronegative substituents.[18] B3LYP/6-31G(d)-optimized structures of these bis(thiocarbonyl)disulfides and their associated radicals $RCS_2^{\cdot}$ are shown in Figure 4, together with selected geometrical parameters. The three disulfides display C_2 molecular symmetry. The S–S bond length in $(Gu^1CS_2)_2$ is markedly longer than the others, at 2.111 Å. Accordingly, the C=S bonds are fairly long (1.664 Å). These structural features suggest that $(Gu^1CS_2)_2$ may have a significantly weaker S–S bond. As in the cases for R = OMe and NMe_2, the C–O and C–N bond lengths in the three disulfides and the corresponding radicals $RCS_2^{\cdot}$ are significantly shorter than the average experimental values (Table 1). Interestingly, the two C–S bonds in $Gu^1CS_2^{\cdot}$ are significantly different in distance (1.717 Å versus 1.684 Å). Careful inspection of the optimized geometry shows that there exists a weak interaction between the sulfur atom characterized by the longer C–S bond with a guanidine nitrogen atom (see Figure 4). The S⋯N separation is 2.453 Å, considerably shorter than the sum of the van der Waal radii (3.40 Å).[34] NBO analysis also reveals that there is strong charge attraction between these two atoms (+0.23 S and −0.53 N). Furthermore, a significant amount of spin density (0.33) is found in this guanidine nitrogen atom. In other words, the radical center is partly delocalized into the guanidine moiety. These unusual structural features described for $Gu^1CS_2^{\cdot}$ are not found in the closely related radical $Gu^2CS_2^{\cdot}$. The greater stabilization of $Gu^1CS_2^{\cdot}$ is confirmed by the computed radical stabilization energies [cf. Eq. (2)]. The stabilization energies of the

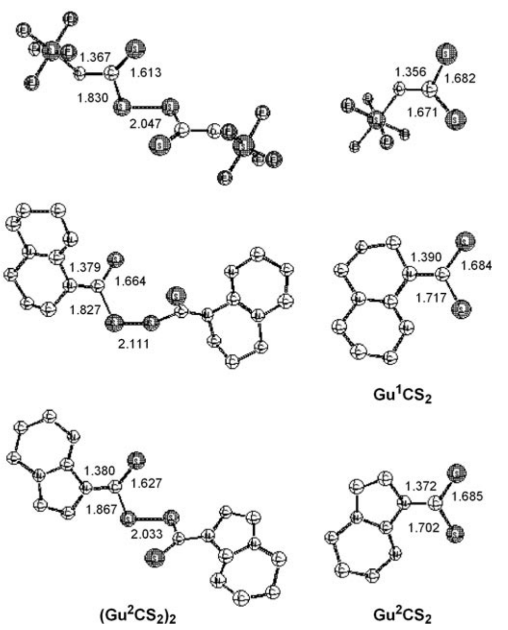

Figure 4. B3LYP/6-31G(d)-optimized structures of $(F_5SOCS_2)_2$, $(Gu^1CS_2)_2$, $(Gu^2CS_2)_2$, $F_5SOCS_2^{\bullet}$, $Gu^1CS_2^{\bullet}$, and $Gu^2CS_2^{\bullet}$. Bond lengths are in Å. Hydrogens are omitted for clarity.

Gu^1 and Gu^2 substituents in the $RCS_2^{\bullet}$ radical are 126.4 and 108.4 kJ mol^{-1} (G3X(MP2) level), respectively.

Homolytic S–S bond dissociation energies (ΔE_0 and ΔH°_{298}) of these three bis(thiocarbonyl)disulfides, calculated at the MP2/6-311+G(d,p)//B3LYP/6-31G(d)+ZPE level, are presented in Table 10. Calculated ΔE_0 and ΔH°_{298} values using this method for R=NMe$_2$ and the corresponding G3X(MP2) values are presented alongside for the purpose of comparison.

Table 10. Calculated reaction energies (ΔE_0 and ΔH°_{298}, kJ mol^{-1}) for the homolytic dissociation $(RCS_2)_2 \rightarrow 2\,RCS_2^{\bullet}$, R=NMe$_2$, OSF$_5$, Gu^1, and Gu^2.

Substituent (R)	MP2/B3LYP[a]		G3X(MP2)	
	ΔE_0	ΔH°_{298}	ΔE_0	ΔH°_{298}
NMe$_2$	150.0	150.0	155.6	155.1
OSF$_5$	188.9	187.7		
Gu^1	115.9	115.4	101.6	102.2
Gu^2	151.4	150.1		

[a] MP2/6-311+G(d,p)//B3LYP/6-31G(d)+ZPE.

For the TMTD case (i.e., R=NMe$_2$), the good agreement between the MP2/6-311+G(d,p) value (149.2 kJ mol^{-1}) and the higher-level G3X(MP2) result (155.6 kJ mol^{-1}) lends us confidence that the MP2 level of theory is an adequate method of choice for studying the energetics of these three larger bis(thiocarbonyl)disulfide systems. As seen from Table 10, the cases for R=OSF$_5$ and Gu^2 are more endothermic than in the TMTD case, by 39.7 and 2.2 kJ mol^{-1}, respectively. Essentially, the effect of the OSF$_5$ group is similar to F, and the Gu^2 substituent behaves like NMe$_2$ (see Table 3). In contrast, the homolytic S–S dissociation reaction $(Gu^1CS_2)_2 \rightarrow 2\,Gu^1CS_2^{\bullet}$ is predicted to be significantly less endothermic, by 33.3 kJ mol^{-1}. The remarkably low S–S BDE of $(Gu^1CS_2)_2$ is confirmed by the higher-level G3X(MP2) calculation (101.6 kJ mol^{-1}). The calculated substituent stabilization energies of Gu^1 in $(RCS_2)_2$ and $RCS_2^{\bullet}$ are 144.5 and 126.4, respectively. Although both values are smaller than the corresponding stabilization energies for the NMe$_2$ substitutent (Table 4), the differential stabilization effect for the bond dissociation process $(RCS_2)_2 \rightarrow 2\,RCS_2^{\bullet}$ is greater for the guanidine-type substituent. In other words, the lower S–S BDE of $(Gu^1CS_2)_2$ is readily attributed to the relatively less stable disulfide $(Gu^1CS_2)_2$. In summary, we predict that $(Gu^1CS_2)_2$ may be a viable alternative to TMTD as a vulcanization reagent, as $Gu^1CS_2^{\bullet}$ radicals can be formed at a lower reaction temperature, which would save costly energy during the vulcanization process.

It is important to examine also the kinetic requirement of the S–S homolysis in these systems. The S–S bond dissociation reaction $(RCS_2)_2 \rightarrow 2\,RCS_2^{\bullet}$ is expected to proceed via a singlet diradical transition state near the point where the singlet potential energy hypersurface (PES) of $(RCS_2)_2$ crosses with the triplet PES of two $RCS_2^{\bullet}$ radicals. Thus, the UB3LYP method was employed to locate the S–S bond dissociation transition states. Higher-level single-point energy calculations were then obtained at the UMP2/6-311+G** level. However, the UMP2 wavefunction is severely spin contaminated in the S–S bond-breaking transition state. A significantly improved UMP2 barrier height was obtained by using a spin correction method developed by Yamaguchi et al.[35] The computed reaction profiles of the S–S homolytic dissociation reaction in $(RCS_2)_2$ for R=NMe$_2$, OSF$_5$, Gu^1, and Gu^2 are summarized in Figure 5.

An activation barrier of 211.2 kJ mol^{-1} is predicted for S–S homolysis of TMTD (R=NMe$_2$). The energy barrier for R=Gu^2 is similar to that in TMTD. In the case of R=OSF$_5$, the barrier is significantly higher at 268.5 kJ mol^{-1}. On the other hand, the activation barrier for R=Gu^1 is calculated

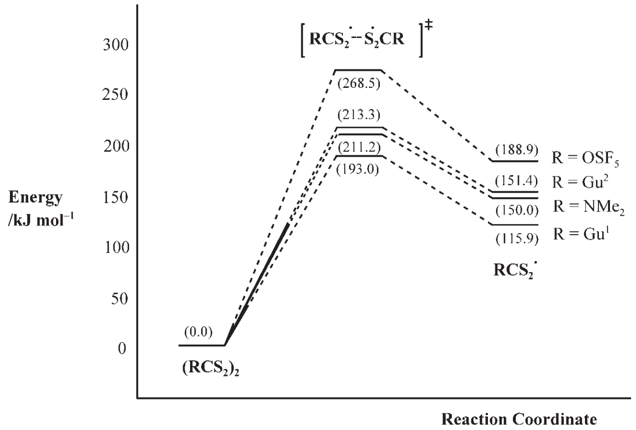

Figure 5. Schematic potential energy profile of the homolytic S–S bond dissociation reaction $(RCS_2)_2 \rightarrow 2\,RCS_2^{\bullet}$, for R=NMe$_2$, OSF$_5$, Gu^1, and Gu^2, calculated at the MP2/6-311+G(d,p)//B3LYP/6-31G(d)+ZPE level of theory. For the transition states, the UMP2 energies were corrected by the spin correction method. Relative energies (kJ mol^{-1}) are given in parentheses.

as 193.0 kJ mol^{-1}, 18.2 kJ mol^{-1} less than that for TMTD. On the basis of the calculated barrier and reaction energy, $(Gu^1CS_2)_2$ is predicted to be more effective than TMTD in providing $RCS_2^{\bullet}$ radicals in the process of rubber vulcanization. Our theoretical finding also provides an avenue to explore the use of highly electron-donating substituents, for instance, polyguanidine-substituted bis(thiocarbonyl)disulfides, as viable reagents in rubber vulcanization. Such efforts would be limited by the size of the substituents themselves, as a bulky group could hinder the cross-linking process instead of promoting it. We hope that our calculations will stimulate further experimental study on the promising system.

Conclusions

The structures and energetics of substituted bis(thiocarbonyl)disulfides $(RCS_2)_2$, their associated radicals $RCS_2^{\bullet}$, and their coordinated compounds with lithium cation, for R = H, Me, F, Cl, OMe, SMe, NMe_2, and PMe_2, have been studied theoretically to determine the effect of substituents on the S–S bond BDE. Most of these $(RCS_2)_2$ molecules have a BDE at about 200 kJ mol^{-1} at the G3X(MP2) level. The effects of substituents on $(RCS_2)_2$ and $RCS_2^{\bullet}$ were analyzed using isodesmic bond exchange reactions. The calculated stabilization energies show pronounced substituent effects on the dimer and its fragmented radical. The stabilization effect is very large for electron-donating groups with an unshared pair of electrons (e.g., OMe and NMe_2). The origin of the significantly lower BDE of TMTD (155 kJ mol^{-1}) can be traced to a differential stabilization of the $Me_2NCS_2^{\bullet}$ radical over the dimer. The addition of Li^+ ion to $(RCS_2)_2$ promotes the homolytic S–S bond dissociation process by providing energy from the exothermic association of Li^+ to $(RCS_2)_2$. This process is likely to proceed by the formation of a triplet complex $[(RCS_2)Li(S_2CR)]^+$; the two $RCS_2^{\bullet}$ radicals are bound to the Li^+ ion through their sulfur atoms in a tetrahedral manner. Additional Li^+ ions would facilitate the process by forming $[Li(S_2CR)]^{\bullet +}$ radicals, and for the TMTD case; this process is by far the most exothermic ($\Delta H^{\circ}_{298} = -206.7$ kJ mol^{-1}). Three novel bis(thiocarbonyl)disulfides with R = OSF_5, Gu^1, and Gu^2 have been explored, and their reaction energies and activation barriers for the homolytic S–S bond dissociation were calculated at the MP2/6-311+G(d,p)//B3LYP/6-31G(d)+ZPE level. Compared to TMTD, both $(F_5SOCS_2)_2$ and $(Gu^2CS_2)_2$ are found to have slightly higher S–S BDEs and larger activation barriers. On the other hand, $(Gu^1CS_2)_2$ shows a promising result, with an S–S BDE of 101.6 kJ mol^{-1} and the corresponding activation barrier of 193.0 kJ mol^{-1}, significantly better than TMTD thermodynamically and kinetically. Thus, $(Gu^1CS_2)_2$ may be an effective reagent in sulfur vulcanization of rubber, which may reduce the reliance on ZnO in reactant mixtures.

Acknowledgement

This work has been supported by the National University of Singapore.

---

[1] D. Hosler, S. L. Burkett, M. J. Tarkanian, *Science* **1999**, *284*, 1988.
[2] M. Akiba, A. S. Hashim, *Prog. Polym. Sci.* **1997**, *22*, 475.
[3] R. Steudel, Y. Steudel, A. M. Mak, M. W. Wong, *J. Org. Chem.* **2006**, *71*, 9302.
[4] S. Kato, M. Nishiwaki, S. Inagaki, S. Ohshima, Y. Ohno, M. Mizuta, T. Murai, *Chem. Ber.* **1985**, *118*, 1684.
[5] A. L. Schroll, G. Barany, *J. Org. Chem.* **1986**, *51*, 1866.
[6] J. Chiefari, R. T. A. Mayadunne, C. L. Moad, G. Moad, E. Rizzardo, A. Postma, M. A. Skidmore, S. H. Thang, *Macromolecules* **2003**, *36*, 2273.
[7] S. H. Thang, Y. K. Chong, R. T. A. Mayadunne, G. Moad, E. Rizzardo, *Tetrahedron Lett.* **1999**, *40*, 2435.
[8] P. Ghosh, *J. Polym. Sci. Part D* **1971**, *5*, 195.
[9] K. J. Klabunde, M. P. Kramer, A. Senning, E. K. Moltzen, *J. Am. Chem. Soc.* **1984**, *106*, 263.
[10] Y. Wang, J. H. Liao, *Acta Crystallogr. Sect. B* **1989**, *45*, 65.
[11] E. J. Suoninen, T. D. Thomas, S. E. Anderson, M. T. Runyan, L. Ungier, *J. Electron Spectrosc. Relat. Phenom.* **1985**, *35*, 259.
[12] L. I. Victoriano, *Coord. Chem. Rev.* **2000**, *196*, 383.
[13] M. Remko, B. M. Rode, *J. Mol. Struct. (THEOCHEM)* **2000**, *505*, 269.
[14] R. Steudel, Y. Steudel, *Chem. Eur. J.* **2006**, *12*, 8589.
[15] L. K. Adams, D. Y. Lyon, P. J. J. Alvarez, *Water Res.* **2006**, *40*, 3527.
[16] S. Hirano, S. Higo, N. Tsukamoto, E. Kobayashi, K. T. Suzuki, *Arch. Toxicol.* **1989**, *63*, 336.
[17] W. S. Beckett, D. F. Chalupa, A. Pauly-Brown, D. M. Speers, J. C. Stewart, M. W. Frampton, M. J. Utell, L.-S. Huang, C. Cox, W. Zareba, G. Oberdörster, *Am. J. Respir. Crit. Care Med.* **2005**, *171*, 1129.
[18] K. Seppelt, *Angew. Chem.* **1982**, *94*, 890; *Angew. Chem. Int. Ed. Engl.* **1982**, *21*, 877.
[19] B. Kovačević, Z. B. Maksić, *Org. Lett.* **2001**, *3*, 1523.
[20] L. A. Curtiss, P. C. Redfern, K. Raghavachari, J. A. Pople, *J. Chem. Phys.* **2001**, *114*, 108.
[21] L. A. Curtiss, P. C. Redfern, K. Raghavachari, V. Rassolov, J. A. Pople, *J. Chem. Phys.* **1999**, *110*, 4703.
[22] A. E. Reed, L. A. Curtiss, F. Weinhold, *Chem. Rev.* **1988**, *88*, 899.
[23] M. Messerschmidt, A. Wagner, M. W. Wong, P. Luger, *J. Am. Chem. Soc.* **2002**, *124*, 732.
[24] Gaussian 03 (Revision C.02), M. J. Frisch, G. W. Trucks, H. B. Schlegel, G. E. Scuseria, M. A. Robb, J. R. Cheeseman, J. A. Montgomery, Jr., T. Vreven, K. N. Kudin, J. C. Burant, J. M. Millam, S. S. Iyengar, J. Tomasi, V. Barone, B. Mennucci, M. Cossi, G. Scalmani, N. Rega, G. A. Petersson, H. Nakatsuji, M. Hada, M. Ehara, K. Toyota, R. Fukuda, J. Hasegawa, M. Ishida, T. Nakajima, Y. Honda, O. Kitao, H. Nakai, M. Klene, X. Li, J. E. Knox, H. P. Hratchian, J. B. Cross, C. Adamo, J. Jaramillo, R. Gomperts, R. E. Stratmann, O. Yazyev, A. J. Austin, R. Cammi, C. Pomelli, J. W. Ochterski, P. Y. Ayala, K. Morokuma, G. A. Voth, P. Salvador, J. J. Dannenberg, V. G. Zakrzewski, S. Dapprich, A. D. Daniels, M. C. Strain, O. Farkas, D. K. Malick, A. D. Rabuck, K. Raghavachari, J. B. Foresman, J. V. Ortiz, Q. Cui, A. G. Baboul, S. Clifford, J. Cioslowski, B. B. Stefanov, G. Liu, A. Liashenko, P. Piskorz, I. Komaromi, R. L. Martin, D. J. Fox, T. Keith, M. A. Al-Laham, C. Y. Peng, A. Nanayakkara, M. Challacombe, P. M. W. Gill, B. Johnson, W. Chen, M. W. Wong, C. Gonzalez, J. A. Pople, Gaussian, Inc., Wallingford, CT, **2004**.
[25] H.-J. Werner, P. Knowles, MOLPRO 2002, University of Birmingham, **2002**.
[26] Experimental bond lengths from Computational Chemistry Comparison and Benchmark Database (CCCBDB) of National Institue of Standards and Technology at http://srdata.nist.gov/cccbdb/.
[27] M. Driess, K. Merz, C. Monsé, *Z. Anorg. Allg. Chem.* **2000**, *626*, 2264.

[28] F. G. N. Cloke, P. B. Hitchcock, P. Hunnable, J. F. Nixon, L. Nyulászi, E. Niecke, V. Thelen, *Angew. Chem.* **1998**, *110*, 1139; *Angew. Chem. Int. Ed.* **1998**, *37*, 1083.
[29] Y. Steudel, M. W. Wong, R. Steudel, *Chem. Eur. J.* **2005**, *11*, 1281.
[30] W. J. Hehre, R. Ditchfield, L. Radom, J. A. Pople, *J. Am. Chem. Soc.* **1970**, *92*, 4796.
[31] Y. Sun, M. W. Wong, *J. Org. Chem.* **1999**, *64*, 9170.
[32] R. Steudel, Y. Steudel, M. W. Wong, *Chem. Eur. J.* **2008**, *14*, 919.
[33] Gu^1 = 1,3,4,6,7,8-hexahydro-2*H*-pyrimido[1,2-*a*]pyrimidine, Gu^2 = 5,6,7,8-tetrahydro-imidazo[1,2-*a*]pyrimidine.
[34] A. Bondi, *J. Phys. Chem.* **1964**, *68*, 441.
[35] S. Yamanaka, T. Kawakami, H. Nagao, K. Yamaguchi, *Chem. Phys. Lett.* **1994**, *231*, 25.

Received: February 5, 2008